npj | climate and atmospheric science

Article

Published in partnership with CECCR at King Abdulaziz University

https://doi.org/10.1038/s41612-025-00976-3

Rising importance of agricultural nitrogen oxide emissions in China's future $PM_{2.5}$ pollution mitigation

Yuanhong Zhao[1,2] ✉, Zhanpeng Su[1,2], Youfan Chen[3], Suyi Hou[1,2], Xiao Lu[4], Bo Zheng[5], Lei Liu[6], Yuepeng Pan[7], Wen Xu[8], Xuejun Liu[8] & Lin Zhang[9] ✉

Controlling ammonia (NH_3) emissions through agricultural management has been recognized as effectively mitigating fine particulate matter ($PM_{2.5}$) pollution in eastern China. However, agricultural nitrogen oxide (NO_x) emissions are often overlooked. Here we estimate agricultural NO_x emissions and design a set of atmospheric chemistry model experiments to assess their role in present and future $PM_{2.5}$ pollution mitigation in eastern China. The results show that when fossil fuel emissions decrease to 2060 levels, the contribution of agricultural NO_x emissions to secondary inorganic aerosol (SIA) concentrations during the crop-growing season will reach 40% over intensive agricultural areas such as North China Plain, and the efficiency of reducing agricultural NO_x emissions in mitigating SIAs will become comparable to reducing NH_3 emissions. By estimating the optimal reactive nitrogen (Nr) emission control pathway, we find that when including agricultural NO_x emissions, the strategies will shift in favor of controlling agricultural Nr emissions to achieve more efficient $PM_{2.5}$ mitigation. Such additional benefits of agricultural nitrogen management should be considered when designing future air quality strategies for agricultural-intensive regions.

Fine particulate matter ($PM_{2.5}$), which describes inhalable particles with an aerodynamic diameter equal to or less than 2.5 μm, is a major pollutant that has been proven to increase susceptibility to respiratory diseases[1]. In China, severe $PM_{2.5}$ pollution contributed to 1.1 million excess deaths in 2015[2]. The anthropogenic emission control strategies implemented by the Chinese government, such as the 'Three-year Action Plan Fighting for a Bule Sky' issued in 2018[3], have significantly reduced $PM_{2.5}$ pollution[4,5]. However, most of the Chinese population is still exposed to $PM_{2.5}$ levels much higher than that recommended by the World Health Organization's Air Quality Guidelines (AQG, annual mean $PM_{2.5}$ of 5 μg m^{-3})[6].

As an important $PM_{2.5}$ precursor, the nitrogen oxides ($NO_x = NO + NO_2$) emissions from combustion sources have been effectively reduced with the implementation of clear air actions in China[7,8]. Besides combustion sources, agricultural soil is also recognized as an important NO_x source and can have a significant influence on ozone air quality[9–11], even in regions that already have a high level of NO_x emissions from fuel combustion, such as North China Plain (NCP)[12–14]. Although the NO_x emissions from agricultural soils are mainly induced by agricultural fertilizer application[14,15], they are usually treated as natural emissions. Recent studies suggest that reducing agricultural NH_3 emissions through agricultural nitrogen management is needed to further control $PM_{2.5}$ pollution in China[15–19]. Agricultural nitrogen management can also reduce NO_x emissions[20]. However, the influence of controlling agricultural NO_x emissions on mitigating $PM_{2.5}$ pollution is rarely recognized in air quality strategies.

The agricultural emissions of NH_3 and NO_x contribute to the formation of secondary inorganic aerosols (sulfate, nitrate, and ammonium

[1]Frontier Science Center for Deep Ocean Multispheres and Earth System (FDOMES) and Physical Oceanography Laboratory, Ocean University of China, Qingdao, China. [2]College of Oceanic and Atmospheric Sciences, Ocean University of China, Qingdao, China. [3]Sichuan Academy of Environmental Policy and Planning, Chengdu, China. [4]School of Atmospheric Sciences, Sun Yat-sen University, Southern Marine Science and Engineering Guangdong Laboratory (Zhuhai), Zhuhai, China. [5]Shenzhen Key Laboratory of Ecological Remediation and Carbon Sequestration, Institute of Environment and Ecology, Tsinghua Shenzhen International Graduate School, Tsinghua University, Shenzhen, China. [6]College of Earth and Environmental Sciences, Lanzhou University, Lanzhou, China. [7]State Key Laboratory of Atmospheric Boundary Layer Physics and Atmospheric Chemistry (LAPC), Institute of Atmospheric Physics, Chinese Academy of Sciences, Beijing, China. [8]College of Resources and Environmental Sciences, National Academy of Agriculture Green Development, Key Laboratory of Plant–Soil Interactions, Ministry of Education, National Observation and Research Station of Agriculture Green Development (Quzhou, Hebei), China Agricultural University, Beijing, China. [9]Department of Atmospheric and Oceanic Sciences, School of Physics, Peking University, Beijing, China. ✉e-mail: zhaoyuanhong@ouc.edu.cn; zhanglg@pku.edu.cn

aerosols, SIAs) through nonlinear chemistry. SO_2 and NO_x emitted to the atmosphere can be oxidized to sulfuric acid (H_2SO_4) and nitric acid (HNO_3), respectively. NH_3 first forms ammonium sulfate aerosol by reacting with H_2SO_4, and then the excess NH_3 will form ammonium nitrate aerosol by reacting with HNO_3. When NH_3 is excessive, which is commonly found in agricultural-intensive areas, controlling NH_3 emissions will first reduce the NH_3 concentrations rather than SIAs[21]. As the SIA formations are more sensitive to HNO_3 than NH_3 over the NH_3-excessive regions, we propose here the effectiveness of controlling agricultural emissions on $PM_{2.5}$ reduction might be underestimated if agricultural NO_x emissions are not considered.

In this study, we investigate the role of agricultural NO_x emissions in mitigating $PM_{2.5}$ pollution during the crop-growing season over eastern China at present and under future scenarios by conducting a set of atmospheric model simulations. We show that over the North China Plain, including agricultural NO_x emissions will shift the optimal reactive nitrogen (Nr) control pathway toward controlling more agricultural emissions and will achieve more effective $PM_{2.5}$ mitigation. Given that most agricultural nitrogen management practices aimed at controlling NH_3 emissions also regulate agricultural NO_x emissions, changes in agricultural NO_x emissions associated with these agricultural management strategies should also be considered when developing emission control strategies for intensive agricultural areas like North China Plain.

Results

Anthropogenic NO_x emissions from agricultural and combustion sectors

Figure 1a and Supplementary Fig. 1 show the spatial distribution and seasonal variation of agricultural NO_x emissions (E_{NOx_agri}) over China in 2019, as estimated by the Berkeley–Dalhousie Soil NO_x Parameterization (BDSNP)[22] with fertilizer application provided by Chen et al.[23] (Supplementary Fig. 2; Methods). The annual total Chinese E_{NOx_agri} estimated by BDSNP is 0.3 Tg N yr^{-1}, consistent with the E_{NOx_agri} given by the sixth Coupled Model Intercomparison Project (CMIP6) scenarios (also 0.3 Tg N yr^{-1}, Methods). The highest agricultural NO_x emissions are found over the North China Plain (NCP), reaching 9 kg N ha^{-1} yr^{-1}, and contributing 35% of the total Chinese agricultural NO_x emission in 2019. In other regions of China, agricultural NO_x emissions are typically less than 1 kg N ha^{-1} yr^{-1}. Significant seasonal variations exist, with the E_{NOx_agri} mainly occurring over May-August, which accounts for 65% of the annual total E_{NOx_agri} (Supplementary Fig. 1). Higher E_{NOx_agri} during May-August can be attributed to high temperature and intensive fertilizer application during these months[10,24].

We evaluate the contribution of E_{NOx_agri} to total anthropogenic NO_x emissions in China in 2019, and the future by comparing with NO_x emissions from combustion sectors (E_{NOx_comb}, including industrial, power plant, transportation, and residential burning) in Fig. 1. The E_{NOx_comb} in 2019 is derived from the Multi-resolution Emission Inventory for China (MEIC)[7,25,26], and in the future (Fig. 1) derived by applying the anthropogenic emission changes (including the agricultural sector) given in the CMIP6 scenarios (Methods). In 2019, the E_{NOx_agri} (0.3 Tg N yr^{-1}) contributes to 5% of annual total anthropogenic NO_x emissions (6.6 Tg N yr^{-1}). In the future, the emission mitigation scenarios in CMIP6 (SSP1-26 and SSP2-45) predict substantial decreases in E_{NOx_comb} but only slight changes in E_{NOx_agri}. The SSP1-26 scenario (strict mitigation pathway scenario), which predicts a sharp reduction of NO_x emissions from industry and transportation, shows E_{NOx_agri} accounting for 11% of the annual total anthropogenic NO_x emissions in 2040 and 27% in 2060. The SSP2-45 scenario (middle road scenario), predicts lower decreases in industry and transportation NO_x emissions compared to the SSP1-26 scenario, resulting in E_{NOx_agri} contributions of 7% in 2040 and 10% in 2060.

The contribution of agricultural NO_x emissions is more significant during the crop-growing season (May-August) (Fig.1 and Supplementary Fig. 3). In 2019, the contribution from E_{NOx_agri} (53 Gg N $month^{-1}$) reached 10% of total anthropogenic NO_x emissions during May-August, which is significantly higher than the residential sector. The E_{NOx_agri} would contribute 43% and 19% of the total anthropogenic NO_x emissions under SSP1-26 and SSP2-45 scenarios in 2060, respectively. Remarkably, under the SSP1-26 scenario, E_{NOx_agri} (50 Gg N $month^{-1}$) during May-August in 2060 would be even higher than the transportation (19 Gg N $month^{-1}$) and industry (31 Gg N $month^{-1}$) sectors, making E_{NOx_agri} a primary contributor to anthropogenic NO_x emissions in China (Supplementary Fig. 3).

The contribution of agricultural NO_x emissions to $PM_{2.5}$ pollution

We use the atmospheric chemistry transport model GEOS-Chem to simulate the $PM_{2.5}$ components in 2019 and the future under SSP2-45 and SSP1-26 scenarios during crop-growing season over East Asia (Methods). The base simulation can generally capture the spatial distribution of the $PM_{2.5}$ concentrations in 2019 observed by the surface network (Supplementary Fig. 4). Our analysis mainly focuses on the SIAs, which are directly impacted by NO_x emissions. The contributions of E_{NOx_agri} and E_{NOx_comb} to SIAs are calculated as the difference between model simulations with all emissions turned on (base simulations in Supplementary Table 1) and simulations with corresponding emissions turned off (sensitivity simulations Group I and II in Supplementary Table 1).

Figure 2 shows the spatial distribution of simulated surface SIA concentrations during the crop-growing season (May-August) of 2019 and under future emission scenarios. In 2019, the model simulated SIA concentrations are more than 20 μg m^{-3} over the majority of eastern China

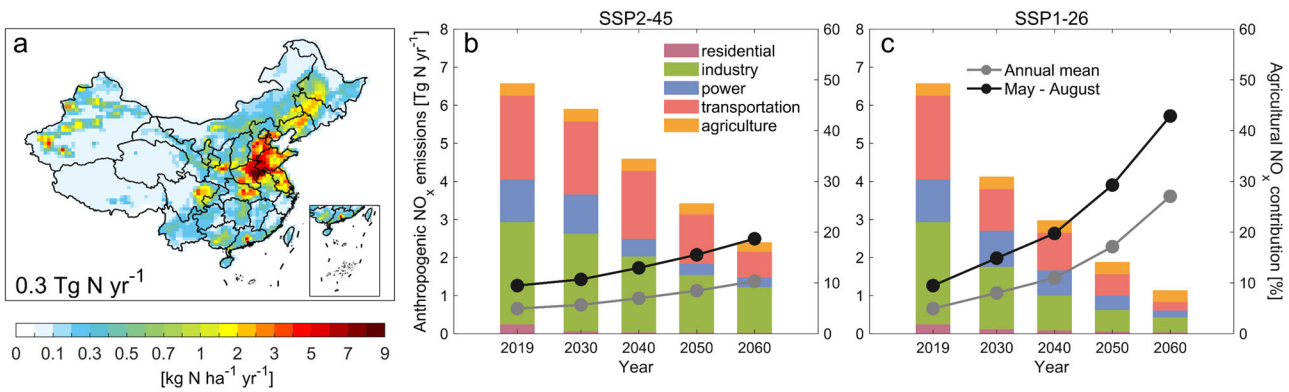

Fig. 1 | The spatial distribution and future changes in agricultural NO_x emissions in China. a The spatial distribution of agricultural NO_x emissions in China was estimated by BDSNP in 2019. The total agricultural NO_x emission over China is shown inset. **b**, **c** The bar plots show the anthropogenic NO_x emissions from each emission sector in 2019 and 2030–2060 under SSP2-45 (**b**) and SSP1-26 (**c**) scenarios (left axis). The lines show the percentage contribution of agricultural NO_x emissions to annual (gray) and May-August (black) total anthropogenic NO_x emissions (right axis).

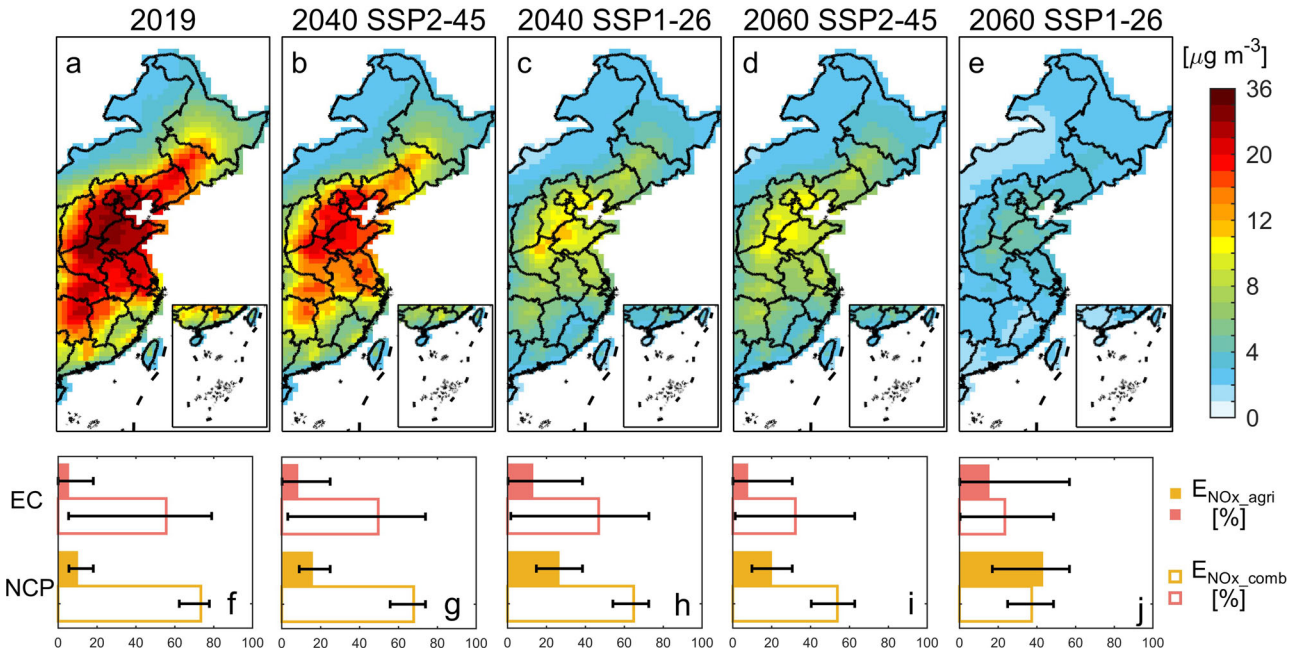

Fig. 2 | The SIA concentrations over eastern China and contribution of agricultural and combustion NO_x emissions. a–e Spatial distribution of SIA concentrations over eastern China simulated by GEOS-Chem averaged over the crop-growing season (May-August) in 2019 (**a**) and under SSP2-45 and SSP1-26 emission scenarios for 2040 and 2060 (**b–e**). **f–j** The corresponding contribution of agricultural NO_x emissions (E_{NOx_agri}) and combustion NO_x emissions (E_{NOx_comb}) to SIA concentrations over East China (EC, red) and North China Plain (NCP, yellow). The bar plots show the median values, and the error bars show the ranges.

except for northeast China and southern coastal regions (5–15 μg m^{-3}). With the reduction of NO_x (Fig. 1) and SO_2 emissions (Supplementary Fig. 5) from combustion sectors, the model simulated significant decreases in SIA concentrations in the future. However, despite these reductions, the formation of SIAs still hinders eastern China from meeting the AQG level (annual mean $PM_{2.5}$ of 5 μg m^{-3})[6]. Under the SSP2-45 scenario, the SIA concentrations are more than 20 μg m^{-3} in 2040 and 10 μg m^{-3} in 2060 over the NCP, implying that SIAs alone (excluding primary aerosols and secondary organic aerosols) could result in $PM_{2.5}$ levels exceeding the AQG level. Under the SSP1-26 scenario, the SIA concentrations in 2060 would decrease to 2–5 μg m^{-3} over most regions of eastern China. Given that SIAs account for 30-50% of $PM_{2.5}$ in eastern China[27–29], further reducing SIAs is essential to ensure $PM_{2.5}$ concentrations below the AQG level.

We compare the contribution of E_{NOx_agri} and E_{NOx_comb} to SIA concentrations over NCP and the whole of eastern China (EC). The spatial distributions of the contribution of E_{NOx_agri} and E_{NOx_comb} to SIA concentrations are shown in Supplementary Fig. 6, and the median values and ranges over NCP and EC are summarized in Fig. 2. The contribution of E_{NOx_agri} to SIA concentrations in 2019 during the crop-growing season is usually below 10% across most regions in eastern China. Over the NCP, where the highest E_{NOx_agri} levels occur, the contribution to surface SIA concentrations reaches about 10-20%. In comparison, the contribution of E_{NOx_comb} can reach more than 50% over most regions in eastern China, much larger than the contribution from E_{NOx_agri}. However, model simulations for future emission conditions indicate a significant increase in the contribution of E_{NOx_agri} to SIAs, particularly over the NCP. In 2060, the E_{NOx_agri} contributions will further increase to 15% over most of eastern China. Over the NCP, the contribution of E_{NOx_agri} will exceed 20% under the SSP2-45 scenario and 40% under the SSP1-26 scenario. Under the SSP1-26 scenario, E_{NOx_agri} contributions will be even larger than those from total E_{NOx_comb}. Additionally, we compare the contributions of E_{NOx_agri} with NO_x emissions from the industrial sector (E_{NOx_ind}), which is the largest combustion source in China (Fig. 1). As shown in Supplementary Fig. 7, under the SSP1-26 scenario, the contribution of E_{NOx_agri} will become roughly equal to that of E_{NOx_ind} from 2040 onwards across eastern China. Over the NCP, the contribution of E_{NOx_agri} will be twice that of E_{NOx_ind} in 2060. Under the SSP2-45 scenario, where industrial emissions are less reduced, the contribution of E_{NOx_agri} will exceed half of E_{NOx_ind} in 2060 over the NCP. Thus, as more stringent measures are expected to be implemented to reduce the emissions from fuel combustion in the future, there will be a growing significance of E_{NOx_agri} in the formation of SIAs. E_{NOx_agri} will serve as a pivotal factor in SIA formations during crop-growing season over eastern China.

The role of controlling agricultural NO_x emissions on $PM_{2.5}$ pollution mitigation

Despite the future reduction of emissions from fossil fuel combustion, eastern China still experiences a substantial level of SIA formations. Since the agricultural emissions show slight changes under the future emission scenarios (Fig. 1 and Supplementary Fig. 8), controlling agricultural emissions could be crucial for further mitigating $PM_{2.5}$ pollution and achieving more stringent air quality targets such as the AQG level[6]. We further evaluate the efficacy of controlling E_{NOx_agri} on $PM_{2.5}$ pollution by comparing the reduction of SIA concentrations resulting from agricultural NH_3 and NO_x emission controls.

Agricultural nitrogen management practices, such as using enhanced-efficiency fertilizers, reducing fertilizer application rate, machine application, and improving manure management, have the potential to reduce NH_3 emissions by ~40%[20,30,31]. A recent study[32] also reported that NH_3 emissions could be mitigated by 49% for wheat and 39% for maize under a county-wide NH_3 reduction campaign in the NCP. In addition to NH_3, agricultural NO_x emissions can also be reduced by about 40% through improved nitrogen management practices[20]. We posit that this potential for a 40% reduction in agricultural NH_3 and NO_x will persist in the future, given the relatively small changes in agricultural emissions predicted by future scenarios (Fig. 1 and Supplementary Fig. 8). Here, we focus our analyses on May as a representative month of the crop-growing season and the results for June-August are shown in the Supplementary Materials.

Figure 3 shows the decline in SIA concentrations resulting from a 40% reduction of agricultural emissions over NCP. The results for the entire eastern China are shown in Supplementary Fig. 9. In May 2019, reducing 40% of agricultural NH_3 emissions would lead to an up to 4.6 μg m^{-3}

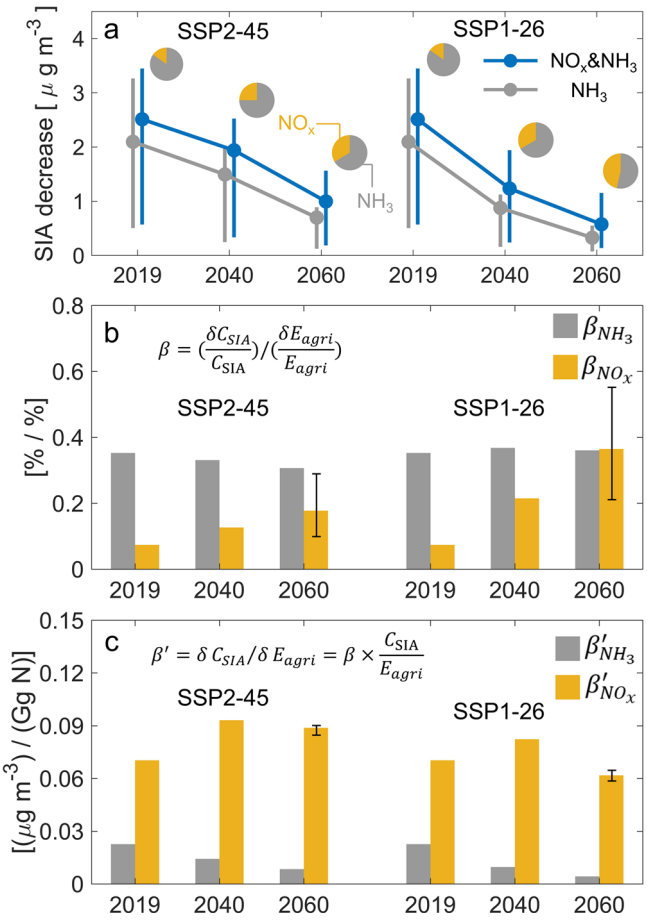

Fig. 3 | The effectiveness of controlling agricultural NO_x and NH_3 emission in SIA mitigation. a The decrease in SIA concentrations in response to a 40% reduction in agricultural NH_3 emissions (gray) and a 40% reduction in both agricultural NH_3 and NO_x emissions (blue) over the North China Plain in May 2019 and under SSP2-45 and SSP1-26 emission scenarios. The solid dots are the median values, and the error bars are the ranges over the North China Plain. The pie plots show the corresponding contribution of population-weighted SIA concentration reductions led by a 40% reduction of agricultural NO_x (yellow) and NH_3 emissions (gray). **b** The efficiency of controlling agricultural NH_3 emissions (β_{NH3}, gray) and agricultural NO_x emissions (β_{NOx}, yellow) in reducing SIA concentrations in May 2019 and under SSP2-45 (left) and SSP1-26 (right) emission scenarios for 2040 and 2060. The error bars show the ranges estimated by assuming a factor of 2 (50–200%) uncertainties in agricultural NO_x emissions. **c** The same as (**b**) but for absolute efficiencies (β'_{NH3} and β'_{NOx}).

decrease in SIA concentrations over eastern China (Supplementary Fig. 9). Over the NCP, where the agricultural emissions are most intensive, the SIA concentrations only decrease by 0.5–3.3 μg m^{-3} (Fig. 3). We estimate the G ratio[33] (Supplementary Text 1) to describe the chemical regime of SIA formations, of which the value large than 1 indicates excessive NH_3 for SIA formations (Supplementary Fig. 10). The limited response of SIA concentrations to NH_3 emission reductions over NCP can be attributed to highly saturated NH_3 simulated by GEOS-Chem sensitivity simulations, where the G values are larger than 1 even with a 40% reduction of E_{NH3_agri}. In the future, the CMIP6 scenarios predict minor changes in agricultural NH_3 emissions (Supplementary Fig. 8). NH_3 will be more excessive in eastern China with reductions of NO_x and SO_2 from fuel combustion under future scenarios (Supplementary Fig. 10), leading to a significant decline in the SIA concentration decreases associated with a 40% reduction in E_{NH3_agri} (Fig. 3). Both the SSP2-45 and SSP1-26 scenarios predict that the corresponding mean SIA decreases in 2060 would be less than 1.0 μg m^{-3} over NCP (Fig. 3).

When both E_{NH3_agri} and E_{NOx_agri} are concurrently reduced by 40%, the response of SIA concentrations to agricultural emission reductions will be more significant than reducing E_{NH3_agri} alone, especially over the NCP (Fig. 3 and Supplementary Fig. 9). This reflects a substantial contribution from E_{NOx_agri} reduction on mitigating SIA formations. In May 2019, E_{NOx_agri} reduction contributed 15% of the overall decrease in SIAs resulting from the total reduction in agricultural Nr (both NH_3 and NO_x) emissions averaged over the NCP (Fig. 3). Under future scenarios, there will be a noticeable increase in the contribution of E_{NOx_agri} (Fig. 3 and Supplementary Fig. 9). By 2060, the contribution of E_{NOx_agri} reduction to the decrease in SIA concentrations led by total agricultural emission reduction is 34% under the SSP2-45 scenario and 46% under the SSP1-26 scenario averaged over the NCP, implying that reducing E_{NOx_agri} by 40% can lead to similar SIA mitigation as E_{NH3_agri}. Over most of the other regions in eastern China, the contribution of E_{NOx_agri} also increases from around 5–15% in 2019 to 20–30% and 30–40% in 2060, respectively, under SSP2-45 and SSP1-26 scenarios (Supplementary Fig. 9).

The rising importance of E_{NOx_agri} can be further quantified using the efficiency of controlling E_{NH3_agri} (β_{NH3}) and E_{NOx_agri} (β_{NOx}) to mitigate SIA formations over NCP[21,34]. Efficiencies β_{NH3} and β_{NOx} are calculated as the ratio of relative changes in population-weighted regional mean SIA concentrations (δC_{SIA}) over the North China Plain to the relative changes in E_{NH3_agri} $\left(\beta_{NH3} = \left(\frac{\delta C_{SIA}}{C_{SIA}}\right)/\left(\frac{\delta E_{NH3\_agri}}{E_{NH3\_agri}}\right)\right)$ and E_{NOx_agri} $\left(\beta_{NOx} = \left(\frac{\delta C_{SIA}}{C_{SIA}}\right)/\left(\frac{\delta E_{NOx\_agri}}{E_{NOx\_agri}}\right)\right)$, respectively. As shown in Fig. 3, in May 2019, β_{NH3} is 0.35%/%, which is about five times of β_{NOx} (0.07%/%). Projecting to future emission scenarios, β_{NH3} shows only slight variations, remaining around 0.35%/%. Different from β_{NH3}, β_{NOx} increases with the reduction of NO_x and SO_2 emissions from combustion sources. In 2060, the β_{NOx} 0.18%/% (0.10–0.29%/% considering a factor of two uncertainty in agricultural NO_x emissions) under SSP2-45 and 0.36%/% (0.21–0.55%/%) under SSP1-26, become comparable to β_{NH3}.

We also calculate the absolute efficiency β'_{NH3} and β'_{NOx} ($\beta'_{NH3} = \delta C_{SIA}/\delta E_{NH3\_agri}$, $\beta'_{NOx} = \delta C_{SIA}/\delta E_{NOx\_agri}$) over NCP in Fig. 3, which describe the SIA changes in response to unit mass changes in agricultural NH_3 and NO_x emissions. β'_{NH3} is much smaller than β'_{NOx}, reflecting the lower sensitivity of SIAs to NH_3 emissions due to the high saturation of NH_3 over the North China Plain. However, the relative efficiency β_{NH3} is higher than β_{NOx}, as agricultural NH_3 emissions are much larger in magnitude compared to NO_x. The decrease of β'_{NH3} reflect that as combustion emissions are reduced, NH_3 becomes more excessive for SIA formation. In 2060, β'_{NOx} is 0.089 μg m^{-3}/Gg N (0.085–0.090 μg m^{-3}/Gg N) and 0.062 μg m^{-3}/Gg N (0.059–0.065 μg m^{-3}/Gg N) for the month of May under SSP2-45 and SSP1-26 scenarios, respectively. In comparison, β'_{NH3} is only 0.008 μg m^{-3}/Gg N under SSP2-45 and 0.004 μg m^{-3}/Gg N under SSP1-26. The model simulations for other months of the crop-growing season under the SSP1-26 scenario in 2060 also show comparable β_{NH3} and β_{NOx} and much higher β'_{NOx} than β'_{NH3} (Supplementary Fig. 11). The results indicate that during the crop-growing season, as NH_3 is saturated for future SIA formations over most of eastern China, the SIA concentrations are projected to be much more sensitive to per unit reduction of E_{NOx_agri} than E_{NH3_agri}.

Implications for future emission control strategies

Choosing an optimal pathway for controlling combustion and agricultural Nr emissions can help achieve the most efficient $PM_{2.5}$ mitigation[34]. As aforementioned, the E_{NOx_agri} are usually treated as natural sources and are not considered in emission control strategies. However, our model sensitivity simulations show that in the future, controlling E_{NOx_agri} can lead to similar SIA reductions to that controlling E_{NH3_agri}. The results imply that E_{NOx_agri} should not be neglected when designing Nr control strategies. Here we further examine the influence of E_{NOx_agri} on the design of efficient emission control pathways for combustion and agricultural reactive nitrogen emissions.

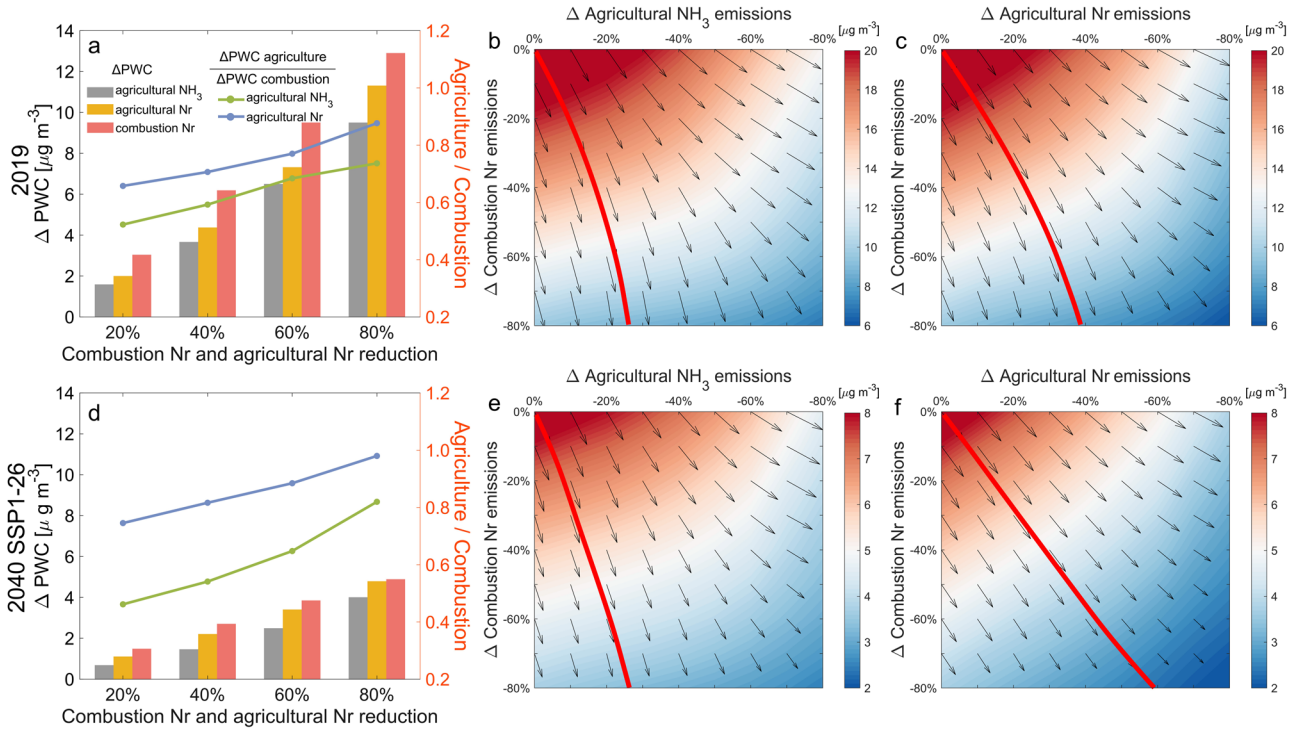

Fig. 4 | Influence of agricultural NO_x emissions on the design of optimal reactive nitrogen emission control pathways over the North China Plain. a, d The bar plots show the decline in population-weighted SIA concentrations (ΔPWC) due to 20–80% reductions in emissions from agricultural NH_3 (gray), agricultural Nr (NO_x and NH_3) (yellow), and combustion Nr emissions (red) (left axis). The blue (green) lines show the ratio of SIAs decrease due to reductions of agricultural Nr (NH_3) and combustion Nr emissions (right axis). **b**, **c**, **e**, **f** Diagrams illustrating the effectiveness of controlling Nr emissions from agricultural and combustion sources in mitigating population SIA concentrations. The background color indicates the population-weighted SIA concentrations over NCP, and the red lines show the optimal emission reduction pathways. Panels (**b**, **e**) are based on estimates that include only agricultural NH_3 emission reductions, while panels (**c**, **f**) include both NH_3 and NO_x emissions in agricultural emission reductions. The arrows indicate the relative magnitude of SIA reductions contributed by reductions in agricultural and combustion reactive nitrogen emissions. The top panels (**a**–**c**) use 2019 emissions, and the bottom panels (**d**–**f**) use emissions reduced to the 2040 level predicted by the SSP1-26 scenario.

To estimate the optimal Nr emission control pathways, we conducted sensitivity simulations Group V-VII, which gradually reduced Nr emissions from agricultural and combustion sources by 20, 40, 60, and 80% (Supplementary Text 2 and Supplementary Table 1). We focus the analysis on NCP during the crop-growing season. To evaluate the influence from E_{NOx_agri}, we estimate the population-weighted regional mean SIA reductions by only reducing E_{NH3_agri} as well as reducing both E_{NH3_agri} and E_{NOx_agri} in the agricultural Nr experiments. In the combustion Nr experiments, we consider the combined reductions in NO_x and NH_3 emissions from combustion sources. These experiments are designed to represent the most simplified case, in which the NH_3 and NO_x are reduced synchronously for each source. The optimal pathway is estimated for 2019 and for the case that the anthropogenic emissions are changed to 2040 levels predicted by the SSP1-26 scenario. The influence from E_{NOx_agri} is evaluated by estimating the optimal pathways with/without including E_{NOx_agri} in agricultural Nr emission control.

We first compare the decline in SIAs due to reducing Nr from combustion sources and agricultural emissions with/without considering E_{NOx_agri}. As shown by Fig. 4a, when ignoring E_{NOx_agri}, the decline in population-weighted regional mean SIA concentrations over NCP due to reducing agricultural Nr emissions is smaller than reducing combustion Nr emissions. We define R as the ratio of SIAs decline due to controlling agricultural and combustion Nr emissions, which represents the relative importance of controlling agricultural Nr emissions in SIA mitigations. We estimate that without considering E_{NOx_agri}, R gradually increased from around 0.5 to 0.8, with the emission reduction increasing from 20 to 80% for both the 2019 and 2040 cases. Such an increase in R reflects that with a deeper reduction in E_{NH3_agri}, the SIA changes from NH_3 saturated to NH_3 limited situation (Supplementary Fig. 12), and the SIA formations will be more sensitive to NH_3 emissions[21]. However, controlling reactive nitrogen emissions from combustion sources is more effective than agricultural emissions ($R < 1$), even with 80% emission reductions. Including E_{NOx_agri} in agricultural Nr emissions reduction can obviously raise the relative importance of controlling agricultural emissions. Particularly, when anthropogenic emissions are reduced to the 2040 level, R for 20% and 80% Nr emission reduction becomes 0.8 and 1.0, making the agricultural Nr emission control able to achieve similar SIA mitigations as combustion Nr for a wide range (20–80%) of Nr emission control process.

We examine the influence of E_{NOx_agri} on designing the optimal Nr emission control pathway following Liu et al.[34] (Supplementary Text 2) in Fig. 4. The optimal pathway is estimated following the direction of the gradients of the SIA concentrations mitigation. If E_{NOx_agri} is not considered, under both 2019 and the 2040 anthropogenic emission conditions predicted by the SSP1-26 scenario, the optimal emission control pathway tends to reduce much more combustion Nr emissions than agricultural NH_3 emissions. The gradients suggest that to achieve the most efficient SIA mitigation, a 20–80% reduction in combustion Nr emissions should be along with 10–26% and 8–26% agricultural NH_3 emissions, respectively, under 2019 and 2040 anthropogenic emissions. Such reduction of Nr emissions will respectively achieve 3.6–13.7 μg m^{-3} and 1.6–5.3 μg m^{-3} population-weighted mean SIA mitigations. When including E_{NOx_agri} reduction, we find that the optimal pathway significantly shifts toward controlling agricultural emissions. Particularly, for the 2040 anthropogenic emission case, we estimate that the agricultural Nr emissions should almost be reduced simultaneously with combustion Nr emission reductions to achieve the most efficient SIA reductions, where the 20–80% reduction in

combustion Nr emissions is suggested along with 14–59% agricultural Nr reduction. The associated population-weighted mean SIA mitigations are increased to 2.0–6.3 μg m^{-3}, which are 16–38% higher than the case that E_{NOx_agri} is neglected.

Discussion

In summary, our study reveals the crucial role of controlling NO_x emissions originating from agricultural activities in mitigating future $PM_{2.5}$ pollution over eastern China during crop-growing season, particularly in regions characterized by intensive agricultural practices, such as NCP. Despite the substantially lower magnitude of agricultural NO_x (0.3 Tg N yr^{-1}) emissions compared to NH_3(8.5 Tg N yr^{-1}), we find that the efficiency of reducing agricultural NO_x emissions in mitigating SIAs will become comparable to reducing NH_3 emissions over the North China Plain when fossil fuel emissions decrease to 2060 levels predicted by future emission scenarios, reflecting the nonlinear chemistry mechanisms of SIA formations. As a result, when designing optimal emission control pathways, including agricultural NO_x emissions will shift the emission control strategies more towards reducing agricultural sources, and will achieve more efficient SIA mitigations.

In this study, we consider a simplified scenario, in which agricultural NO_x and NH_3 are synchronously controlled. This assumption is reasonable for a quick evaluation of the implications of agricultural NO_x emissions on emission control strategies, since most of the nitrogen management practices, such as reducing the overuse of chemical fertilizer, can collectively reduce NH_3 and NO_x emissions. By synthesizing a wealth of field measurements, previous studies have summarized the impact of 11 different reactive nitrogen management practices on nitrogen loss[20]. These practices vary in terms of technical thresholds, mitigation efficacy, and implementation costs. Most of the practices affect both NH_3 and NO_x emissions, but the reduction in NH_3 and NO_x emissions in response to a single practice can differ significantly (Supplementary Table 2). For example, using enhanced-efficiency fertilizers can reduce NH_3 emissions by 69% and NO_x emissions by 46%, while irrigation management (e.g., reduced irrigation or drip irrigation) can reduce NH_3 emissions by 36% and NO_x emissions by 93%[20]. The increased contribution of agricultural NO_x emissions does not only occur in Eastern China. As predicted by SSP scenarios, over the anthropogenic emissions hotspots, such as India, Southeast Asia, and Western Europe, the contribution of agricultural sources to total anthropogenic sources will reach ~20% by 2060, similar to the contribution over Eastern China (Supplementary Fig. 13). Thus, to meet more stringent air quality standards and achieve continuous air quality improvement over agricultural-intensive areas in Eastern China and in other regions, we call for a detailed consideration of how nitrogen management practices can influence agricultural NO_x emissions for designing future agricultural emission control strategies.

Methods

GEOS-Chem model description

We use the global three-dimensional chemistry transport model GEOS-Chem (version 12.9.3) to simulate the $PM_{2.5}$ concentrations and their response to emission changes over China during the crop-growing season in 2019. We use the nested version of GEOS-Chem with a horizontal resolution of 0.625°(longitude) × 0.5°(latitude) over East Asia and 2.5°(longitude) × 2°(latitude) over the rest of the world. The model incorporates a comprehensive state-of-the-art O_3-NO_x-hydrocarbon-aerosol-halogen chemistry in the troposphere[35,36]. To estimate the partition of gas phase H_2SO_4-HNO_3-NH_3 with SIAs, the model employed the ISORROPIA-II thermodynamical model[37]. The chemistry, transportation, and deposition of chemical species as well as the biogenic emissions including soil NO_x are driven by MERRA-2 meteorological data provided by the Global Modeling and Assimilation Office (GMAO) at the National Aeronautics and Space Administration (NASA). The MERRA-2 data has a temporal resolution of 1 h for surface variables and boundary layer height and 3 h for other three-dimensional variables.

The anthropogenic emissions other than agricultural NH_3 over China are from the Multi-resolution Emission Inventory for China (MEIC; http://meicmodel.org/)[7,38]. The agricultural NH_3 emissions are from the bottom-up emission inventory given by Zhang et al.[7] and Chen et al.[23]. The natural emissions include NO_x emissions from soil estimated by the Berkeley–Dalhousie Soil NO_x emission Parameterization (BDSNP)[22] and from lightning parameterized based on the cloud-top height[39], biogenic volatile organic compound (VOC) emissions estimated by the Model of Emissions of Gases and Aerosols from Nature (MEGAN v2.1) algorithm[40], and biomass burning given by the Global Fire Emissions Database version 4 (GFED4)[41]. By employing the aforementioned emission inventories, the model can generally capture the spatial distribution of $PM_{2.5}$ concentration over China during the crop-growing season (May-August) when compared with the surface observations collected from the Ministry of Ecology and Environment of China (Supplementary Fig. 4).

Agricultural NO_x emission parameterization

The agricultural NO_x emissions are estimated as a part of soil NO_x emissions by the BDSNP that was implemented in GEOS-Chem[22]. This parameterization characterizes the soil NO_x emissions by considering the available soil nitrogen as well as meteorological conditions, including temperature and water-filled pore space (defined as the ratio of volumetric soil water content to total soil porosity). The dependence of agricultural NO_x emissions on soil organic matter[42] is not included in BDSNP parameterization. The BDSNP also considers the pulse of soil NO_x emissions when the water-stressed bacteria is reactivated by irrigation or rainfalls and the canopy uptake of NO_x. Lu et al.[12] have demonstrated that the BDSNP parameterization can generally capture the spatial distribution of soil NO_x emission in China when compared with available field measurements and satellite observation of tropospheric NO_2 column density.

The available soil nitrogen includes the natural nitrogen pool as well as the external nitrogen input from fertilizer application and atmospheric deposition. Thus, agricultural NO_x emissions can be calculated using the BDSNP parameterization by distinguishing the soil NO_x emissions resulting from fertilizer nitrogen input. In Hudman et al.[22], the spatial distribution of chemical fertilizer and manure is from Potter et al.[43], with 37% of the manure added to soil nitrogen content. Since Potter et al.[43] estimated the chemical fertilizer application and manure based on data reported from 1994 to 2001, we updated the dataset based on Chen et al.[23], which estimated the monthly chemical fertilizer and manure for China between 2005 and 2016. Unlike the assumption made by Hudman et al.[22] that 75% of the fertilizer is applied around the green-up day, Chen et al.[23] considered detailed fertilizer application practices in China. In addition, the manure applied to the soil is estimated by the process-based mass-flow method. Annually, the total fertilizer application (chemical fertilizer and manure applied to soil) from Chen et al.[23] (35 Tg yr^{-1}) is higher than that given by Potter et al.[43] (Supplementary Fig. 2). Besides direct fertilizer application, agricultural activities also indirectly contribute to soil nitrogen content through enhanced atmospheric deposition of reactive nitrogen. Through a sensitivity simulation that turns off all agricultural reactive nitrogen emissions, we estimate that soil NO_x emissions driven by agricultural-induced nitrogen deposition account for only 3% of those from direct fertilizer application. Using the BDSNP parameterization, we calculate total soil NO_x emissions in China to be 0.68 Tg N yr^{-1}, of which 0.33 Tg N is induced by agricultural fertilizer application, identified as agricultural NO_x emissions in this study. The agricultural NO_x emissions in China calculated with the updated fertilizer input data are 43% higher than the estimate obtained using the original BDSNP parameterization (Supplementary Fig. 14). The largest differences are observed over the North China Plain, where our updated estimates can exceed the original BDSNP by as much as 4 kg N ha^{-1} yr^{-1}.

Future emission scenarios

We investigate the contribution of agricultural NO_x emissions on $PM_{2.5}$ pollution in the future based on the anthropogenic emission changes given by the sixth Coupled Model Intercomparison Project (CMIP6) scenarios[44]. The

CMIP6 scenarios encompass projections of climate forcing in 2100 and future social evolutions by linking the Representative Concentration Pathways (RCPs) with the Shared Socioeconomic Pathways (SSP1-5). The Tier 1 scenarios of CMIP6 provide a comprehensive range of future climate-forcing targets, which include two baseline scenarios (SSP3-70 and SSP5-85) and two mitigation scenarios (SSP1-26 and SSP2-45). In this study, we chose the emission mitigation scenarios taking into account emission control policies in China. The SSP2-45 and SSP1-26 present a middle road and a strict mitigation pathway scenario, respectively. We only apply the annual scale factor for each emission sector estimated for the integrated assessment model (IAM) regions[44] to GEOS-Chem emissions to represent future anthropogenic emission changes under various climate targets and emission control strategies.

Model experiments

We investigate the role of agricultural NO_x emissions on $PM_{2.5}$ pollution over eastern China through a series of GEOS-Chem model experiments as listed in Supplementary Table 1. The base simulations use the anthropogenic emission inventories described above, and future $PM_{2.5}$ changes use the anthropogenic emissions for 2040 and 2060 predicted by SSP2-45 and SSP1-26 scenarios. To assess the contribution of agricultural and combustion NO_x emissions to $PM_{2.5}$ pollution, we conduct sensitivity simulations Group I and II, which are the same as base simulations but turn off agricultural NO_x emissions and combustion NO_x emissions, respectively. We further examine the role of agricultural NO_x emissions in controlling present and future $PM_{2.5}$ pollution by conducting simulations sensitivity simulations in Groups III and IV. Compared with the standard simulations, simulations in Group III reduce agricultural NH_3 emissions by 40%, and simulations in Group IV reduce both agricultural NH_3 and NO_x emissions by 40%. To evaluate how the uncertainties in E_{NOx_agri} will influence the efficiency of controlling agricultural NO_x on mitigating SIA concentrations in the future, we also conduct simulations that assume a factor of 2 uncertainty (50–200%) in E_{NOx_agri} following Lu et al.[12] for sensitivity simulations Group III and IV for 2060. To estimate the optimal reactive Nr emission control pathways, we conduct sensitivity simulations in Groups V, VI, VII, which gradually reduce the Nr emissions from agricultural/combustion sources by each 20% step. We calculate the population-weighted regional mean SIA concentrations (PWC) based on the gridded SIA concentrations ($C_{SIA,i,j}$) and the corresponding population densities ($P_{i,j}$) from LandScan Global 2019[45] .

$$\mathrm{PWC} = \frac{\sum_{i,j} C_{\mathrm{SIA},i,j} \times P_{i,j}}{\sum_{i,j} P_{i,j}}$$

We should note here since we only focus on the changes in anthropogenic emissions, all above simulations are conducted with the meteorological conditions fixed to 2019. The uncertainties from emissions and meteorological conditions are discussed in the Supplementary Materials.

Data availability

Surface $PM_{2.5}$ measurements in China are available at https://air.cnemc.cn/. The MEIC emissions are available at https://meicmodel.org.cn/. The CMIP6 emissions are available at https://tntcat.iiasa.ac.at/SspDb/. Modeling outputs are available from the corresponding author upon reasonable request.

Code availability

The GEOS-Chem model code and descriptions are available at http://wiki.seas.harvard.edu/geos-chem/index.php/Main_Page.

Received: 16 December 2024; Accepted: 20 February 2025;
Published online: 07 March 2025

References

1. Yang, L., Li, C. & Tang, X. The impact of PM(2.5) on the host defense of respiratory system. *Front. Cell Dev. Biol.* **8**, 91 (2020).
2. Cohen, A. J. et al. Estimates and 25-year trends of the global burden of disease attributable to ambient air pollution: an analysis of data from the Global Burden of Diseases Study 2015. *Lancet* **389**, 1907–1918 (2017).
3. State Council of the People's Republic of China (SC). Notice of the State Council on Issuing the Three-year Action Plan Fighting for a Blue Sky. (2018)
4. Zhai, S. et al. Fine particulate matter (PM2.5) trends in China, 2013–2018: separating contributions from anthropogenic emissions and meteorology. *Atmos. Chem. Phys.* **19**, 11031–11041 (2019).
5. Zhang, Q. & Geng, G. Impact of clean air action on PM2.5 pollution in China. *Sci. China Earth Sci.* **62**, 1845–1846 (2019).
6. Organization, W. H. *WHO Global Air Quality Guidelines: Particulate Matter (PM2. 5 and PM10), Ozone, Nitrogen Dioxide, Sulfur Dioxide and Carbon Monoxide* (World Health Organization, 2021).
7. Zheng, B. et al. Trends in China's anthropogenic emissions since 2010 as the consequence of clean air actions. *Atmos. Chem. Phys.* **18**, 14095–14111 (2018).
8. Li, H. et al. Trends and drivers of anthropogenic NOx emissions in China since 2020. *Environmental Science Ecotechnology* **21**, 100425 (2024).
9. Romer, P. S. et al. Effects of temperature-dependent NOx emissions on continental ozone production. *Atmos. Chem. Phys.* **18**, 2601–2614 (2018).
10. Oikawa, P. Y. et al. Unusually high soil nitrogen oxide emissions influence air quality in a high-temperature agricultural region. *Nat. Commun.* **6**, 8753 (2015).
11. Almaraz, M. et al. Agriculture is a major source of NOx pollution in California. *Sci. Adv.* **4**, eaao3477 (2018).
12. Lu, X. et al. The underappreciated role of agricultural soil nitrogen oxide emissions in ozone pollution regulation in North China. *Nat. Commun* **12**, 5021 (2021).
13. Wang, R. et al. Cropland nitrogen dioxide emissions and effects on the ozone pollution in the North China plain. *Environ. Pollut.* **294**, 118617 (2022).
14. Shen, Y. et al. Impacts of agricultural soil NOx emissions on O_3 over mainland China. *J. Geophys. Res. Atmos.* **128**, e2022JD037986 (2023).
15. Gu, B. et al. Abating ammonia is more cost-effective than nitrogen oxides for mitigating PM2.5 air pollution. *Science* **374**, 758–762 (2021).
16. Guo, H. et al. Effectiveness of ammonia reduction on control of fine particle nitrate. *Atmos. Chem. Phys.* **18**, 12241–12256 (2018).
17. Xu, Z. et al. High efficiency of livestock ammonia emission controls in alleviating particulate nitrate during a severe winter haze episode in northern China. *Atmos. Chem. Phys.* **19**, 5605–5613 (2019).
18. Han, X., Zhu, L., Liu, M., Song, Y. & Zhang, M. Numerical analysis of the impact of agricultural emissions on PM2.5 in China using a high-resolution ammonia emissions inventory. *Atmos. Chem. Phys*. **20**, 1–31 (2020).
19. Liu, M. et al. Ammonia emission control in China would mitigate haze pollution and nitrogen deposition, but worsen acid rain. *Proc. Natl Acad. Sci. USA* **116**, 7760–7765 (2019).
20. Gu, B. et al. Cost-effective mitigation of nitrogen pollution from global croplands. *Nature* **613**, 77–84 (2023).
21. Liu, Z. et al. The nonlinear response of fine particulate matter pollution to ammonia emission reductions in North China. *Environ. Res. Lett.* **16**, 034014 (2021).
22. Hudman, R. C. et al. Steps towards a mechanistic model of global soil nitric oxide emissions: implementation and space based-constraints. *Atmos. Chem. Phys.* **12**, 7779–7795 (2012).
23. Chen, Y. et al. Interannual variation of reactive nitrogen emissions and their impacts on PM 2.5 air pollution in China during 2005-2015. *Environ. Res. Lett.* **16**, 125004 (2021).
24. Zhang, L. et al. Agricultural ammonia emissions in China: reconciling bottom-up and top-down estimates. *Atmos. Chem. Phys.* **18**, 339–355 (2018).

25. Li, M. et al. MIX: a mosaic Asian anthropogenic emission inventory under the international collaboration framework of the MICS-Asia and HTAP. *Atmos. Chem. Phys.* **17**, 935–963 (2017).
26. Zheng, B. et al. Changes in China's anthropogenic emissions and air quality during the COVID-19 pandemic in 2020. *Earth Syst. Sci. Data* **13**, 2895–2907 (2021).
27. Zhao, P. S. et al. Characteristics of concentrations and chemical compositions for $PM_{2.5}$ in the region of Beijing, Tianjin, and Hebei, China. *Atmos. Chem. Phys.* **13**, 4631–4644 (2013).
28. Huang, R.-J. et al. High secondary aerosol contribution to particulate pollution during haze events in China. *Nature* **514**, 218–222 (2014).
29. Sun, Y. et al. Rapid formation and evolution of an extreme haze episode in Northern China during winter 2015. *Sci. Rep.* **6**, 27151 (2016).
30. Guo, Y. et al. Air quality, nitrogen use efficiency and food security in China are improved by cost-effective agricultural nitrogen management. *Nat. Food* **1**, 648–658 (2020).
31. Liu, L. et al. Exploring global changes in agricultural ammonia emissions and their contribution to nitrogen deposition since 1980. *Proc. Natl Acad. Sci. USA* **119**, e2121998119 (2022).
32. Kang, J. et al. Ammonia mitigation campaign with smallholder farmers improves air quality while ensuring high cereal production. *Nat. Food* **4**, 751–761 (2023).
33. Ansari, A. S. & Pandis, S. N. Response of inorganic PM to precursor concentrations. *Environ. Sci. Technol.* **32**, 2706–2714 (1998).
34. Liu, Z. et al. Optimal reactive nitrogen control pathways identified for cost-effective PM2.5 mitigation in Europe. *Nat. Commun.* **14**, 4246 (2023).
35. Park, R. J., Jacob, D. J., Field, B. D., Yantosca, R. M. & Chin, M. Natural and transboundary pollution influences on sulfate-nitrate-ammonium aerosols in the United States: implications for policy. *J. Geophys. Res. Atmos.* **109** (2004).
36. Mao, J. et al. Chemistry of hydrogen oxide radicals (HOx) in the Arctic troposphere in spring. *Atmos. Chem. Phys.* **10**, 5823–5838 (2010).
37. Fountoukis, C. & Nenes, A. ISORROPIA II: a computationally efficient thermodynamic equilibrium model for K^+–Ca^{2+}–Mg^{2+}–NH_4^+–Na^+–SO_4^{2-}–NO_3^-–Cl^-–H_2O aerosols. *Atmos. Chem. Phys.* **7**, 4639–4659 (2007).
38. Li, M. et al. Anthropogenic emission inventories in China: a review. *Natl Sci. Rev.***4**, 834–866 (2017).
39. Murray, L. T., Jacob, D. J., Logan, J. A., Hudman, R. C. & Koshak, W. J. Optimized regional and interannual variability of lightning in a global chemical transport model constrained by LIS/OTD satellite data. *J. Geophys. Res. Atmos.* **117**, D20307 (2012).
40. Guenther, A. B. et al. The model of emissions of gases and aerosols from nature version 2.1 (MEGAN2.1): an extended and updated framework for modeling biogenic emissions. *Geosci. Model Dev.* **5**, 1471–1492 (2012).
41. Randerson, J. T., Van Der Werf, G. R., Giglio, L., Collatz, G. J. & Kasibhatla, P. S. *Global Fire Emissions Database, Version 4.1* (*GFEDv4*) (ORNL Distributed Active Archive Center, 2017).
42. Liu, X. et al. NO and N2O fluxes from agricultural soils in Beijing area. *Prog. Nat. Sci.* **14**, 489–494 (2004).
43. Potter, P., Ramankutty, N., Bennett, E. M. & Donner, S. D. Characterizing the spatial patterns of global fertilizer application and manure production. *Earth Interact.* **14**, 1–22 (2010).
44. Gidden, M. J. et al. Global emissions pathways under different socioeconomic scenarios for use in CMIP6: a dataset of harmonized emissions trajectories through the end of the century. *Geosci. Model Dev.* **12**, 1443–1475 (2019).
45. Rose, A. et al. *LandScan Global 2019* (Oak Ridge National Laboratory, 2020).

Acknowledgements

This research was supported by Shandong Provincial Natural Science Fund for Excellent Young Scientists Fund Program (Overseas) (grant no. 2022HWYQ-066), Shandong Provincial Natural Science Foundation (grant no. ZR2021QD117), National Natural Science Foundation of China (grant no. 42305101), the China Postdoctoral Science Foundation (2022M712985). The numerical calculations in this paper have been done at Hefei advanced computing center.

Author contributions

Y.Z. and L.Z. designed the study. Z.S., Y.Z., and S.H. performed the model simulations and analyzed data. Y.C. provided the fertilizer application data. Y.Z., L.Z., and Z.S. wrote the article with valuable comments from all authors.

Competing interests

The authors declare no competing interests.

Additional information

Supplementary information The online version contains supplementary material available at https://doi.org/10.1038/s41612-025-00976-3.

Correspondence and requests for materials should be addressed to Yuanhong Zhao or Lin Zhang.